



Transactions of the 13th International Conference on Structural Mechanics in Reactor Technology (SMiRT 13), Escola de Engenharia - Universidade Federal do Rio Grande do Sul, Porto Alegre, Brazil, August 13-18, 1995

### 3D nonlinear finite element analysis of elbows with surface cracks

Maeda, O.<sup>1</sup>, Satoh, Y.<sup>1</sup>, Fukuda, Y.<sup>1</sup>, Ohno, K.<sup>2</sup>, Dozaki, K.<sup>2</sup>

1) Hitachi Ltd., Hitachi, Japan

2) The Japan Atomic Power Company, Tokyo, Japan

#### Abstract

This paper shows 3D/FEM estimations of surface crack propagation behavior in an elbow under cyclic in-plane bending load conditions. Elastic-plastic analyses and creep analyses were performed for surface cracks in the elbow. The integrals of  $J$  and  $J'$  were calculated by using the VCE method and the integral path method, respectively. The material of the elbows used was 316FR stainless steel. Their thickness, diameter, and bend radius were 15.9 mm, 965.2 mm, and 965.2 mm, respectively. Initial surface cracks were semielliptical; initial crack lengths ( $2c_0$ ) were 15.9 mm in the short crack, and 350 mm and 700 mm in the hypothetical long crack, and initial crack depths ( $a_0$ ) were 3.2 mm to 8.0 mm. From the analytical results, the distributions of the  $J$ -integral along the crack front, showed the following tendencies; in the short crack of the aspect ratio  $a/c = 1/2.5$ , a crack propagates in the direction both the depth and the length, while in a long crack of the aspect ratio  $a/c = 1/55$ , a crack propagates in the depth direction only. These surface propagation tendencies agree well with results of experiments on a crack of similar shape.

#### 1. Introduction

In recent years, extensive studies using non-linear fracture mechanics have been carried out on crack propagation under low cycle fatigue conditions with macroscopic plastic deformations. These studies have indicated that the cyclic  $J$  integral, a nonlinear fracture mechanics parameter, can predict fatigue crack propagation behavior. However, because the  $J$ -integral depends on material nonlinearity and crack closure and analysis of the cyclic  $J$ -integral is very complex, few closed-form formulas can be used to estimate the  $J$ -integral for three dimensional (3D) cracks contained in components of industrial machinery.

Therefore, a numerical analysis such as the finite element method (FEM) is needed to estimate the  $J$ -integral for 3D structures.

But there are a few examples such as having a complicated 3D shape like an elbow subjected to a bending load.<sup>(1)</sup> The  $J'$ -integral is also necessary for calculating creep fatigue crack propagation in elevated temperature structure components.<sup>(1)</sup> The  $J$ -integral depending on FEM analysis of an elbow with surface crack was desired to have correct value and was necessary to review it comparatively with the  $J$ -integral that we calculate by a simplified shape for LBB (leak before break) evaluation of Japanese DFBR (demonstration fast breeder reactor) piping. For these reasons, the  $J$  and  $J'$  integrals were calculated by means of primary heat transport system piping of DFBR by using a detailed 3D FEM analytic model. Two types of crack sizes were selected. One was a short crack dimension (length  $2C_0 = 1.0 t$ , depth  $a_0 = 0.2 t$ , where  $t$  is thickness) and the other was a hypothetical long crack; that is to grasp the application limits of the simplified estimation method. We compared the  $J$ -integral distribution result with a similar shape crack propagation experimental result of an elbow<sup>(2)</sup> and also compared it with a result obtained using simplified estimation method.<sup>(3)</sup>

## 2. Analytical procedure

In order to obtain the J-integral of a 3D surface crack of an elbow subjected to an in-plane bending load at elevated temperatures, six cases of elastic-plastic analyses and a creep analysis were performed using the detail finite element method. In these analyses, the analytical code SIMUS (simulation program for multilayer structure) <sup>(4)</sup> which was developed by HITACHI, was used.

### 2.1 Analytical model and analysis cases

The analytic object was L-shaped piping with a 90° elbow connecting two straight pipes, as shown in Fig. 1. The material of the tested elbows was 316FR stainless steel. Their thickness, diameter, and bend radius were 15.9 mm, 965.2 mm, and 965.2 mm, respectively. Analyses were performed for in-plane bending, considering the dimension of a surface crack as a parameter, and enforced an elastic-plastic analysis, elastic-plastic creep analysis about six cases of crack dimensions, as shown in Table 1. We assumed superficial cracks for both elbow sides axially on the crown inside  $\theta = 95^\circ$  and  $\theta = 175^\circ$  sections where maximum stress occurs.

To determine boundary conditions for an applied load, displacement was calculated by the following means. First, the relation between displacement and the strain amplitude  $\varepsilon$  of the above-mentioned maximum point was calculated in a crackless state by elastic analysis.

Then displacement  $u = 22$  mm was determined by  $\varepsilon = 0.18\%$  for elastic-plastic analyses and creep analyses for each crack. The number of steps in the analysis was 11 for an elastic-plastic analysis and the auto-creep function step of that program in a creep analysis. The creep time was used 800 hr in cases 1 to 3 and 280 hr in cases 4 and 5. In analysis case 6 was enforced elastic-plastic analysis only. For symmetry of load and configuration, the analytic model was at 1/4 scale. Fig. 2 shows element meshes of case 4 as an example. The displacement  $u$  was given at the point of the lower most edge of the analytic model and an caused in-plane bending moment.

A three-dimensional isoparametric solid element with 20 nodes and  $3 \times 3 \times 3$  integral points was used. A representative point position of a strain calculation was the nearest inside integral point to  $\theta = 95^\circ$  section that contained a crack.

### 2.2 Material constants for analysis

The material constants was used as Poisson's ratio  $\nu = 0.306$ , the Young's modulus  $E = 15700$  kg/mm<sup>2</sup>, at 550 °C,  $\alpha$ ,  $\sigma_0$ ,  $\varepsilon_0$  and  $n$  were the constants when the stress-strain diagram was represented as a Ramberg-Osgood approximation with the following equation:

$$\frac{\varepsilon_p}{\varepsilon_0} = \alpha \left( \frac{\sigma}{\sigma_0} \right)^n \quad \text{where } \varepsilon_0 = 5.97 \times 10^{-4}, \sigma_0 = 9.36 \text{ kgf/mm}^2, \\ \varepsilon_p \text{ is plastic strain, } \sigma \text{ is stress, and } \alpha = 0.131, \\ n = 3.44.$$

Norton's relation was used as a creep law:

$$\dot{\varepsilon}_c = 2.815 \times 10^{-25} \times \sigma_M^{13.017}$$

where  $\dot{\varepsilon}_c$  is creep strain rate in kgf/mm<sup>2</sup> and  $\sigma_M$  is Mises's equivalent stress in kgf/mm<sup>2</sup>.

### 2.3 J-integral path

The J and J' integrals were calculated by the VCE (virtual crack extension) method and the route integral method, respectively. The integral paths and finite element mesh for the J-integral based on an elastic-plastic analysis is shown in Fig. 3. Also, the integral paths and finite element mesh for the J-integral on creep analysis is shown in Fig. 4.

### 2.4 Calculation results for the J-integral

The J-integral distribution corresponding to the crack front for cases 1 and 4 is shown in Figs. 5 and 6. In case 1 as an example of a short crack, though the J-integral at the central point of the crack is the largest, the crack end point is half the value of the central point of the crack, and the tendency of propagation shows directions of both depth and length. In case 4 as an analytical case of a hypothetical long crack compared to a short crack, the J-integral at the

central point of the crack and also the neighboring value is the largest, and the  $J$ -integral at a crack end point is extremely small, showing that the crack has a tendency to propagate only in the depth direction. The  $J$ -integrals corresponding to the crack fronts of every case investigated by FEM analysis are shown in Table 1. In this table, the  $J$ -integral of the central point of the crack is shown as  $J_a$ , and as the end point of the crack as  $J_c$ . The  $J'$ -integral distribution corresponding to the crack front for cases 1 and 4 are shown in Figs. 7 and 8. In the analysis of case 1, with a short crack, the  $J'$ -integral at the central point of the crack is large, showing a tendency to propagate in the directions of both depth and length. Against this, in analytic case 4, for a hypothetical long crack, the  $J'$ -integral at a central neighboring point of the crack is the largest on contraction, becoming an extremely small value at the crack end point, and showing a tendency to propagate in the depth direction.

### 3. Simplified evaluation for crack propagation

#### 3.1 Simplified estimation method

The  $J$ -integral was calculated by the simplified estimation method (known as the Detail Parameter Method<sup>(3)</sup>). This method can present the  $J$ -integrals at the surface end and the maximum depth point of a surface crack analytical equations introduced from the result of finite element analysis on the surface cracked plate specimen. The equations are expressed as the function of crack length ( $c$ ), crack depth ( $a$ ), plate thickness ( $t$ ) and plate width ( $2W$ ) for bending loads. A wide range of configuration parameters was included in the equations.

We confirmed that the ratio aspect agrees well with the FEM analytic value of a flat plate, about a short crack to  $a/c = 1/8$ . The verification of these result is shown for Fig. 9.<sup>(3)</sup> The application range of this simplified estimation method is  $0 < a/c \leq 1.0$ ,  $0 < a/t < 0.75$ ,  $c/W \leq 0.8$ , and we confirmed analytically an aspect ratio range of  $1/16 \leq a/c \leq 1/2$ .

#### 3.2 Calculation results of the $J$ -integral by the simplified estimation method

The  $J$ -integral at a central point of the crack ( $J_a$ ) and crack end point ( $J_c$ ) were calculated for the same geometry of detailed FEM analysis model of an elbow. A strain amplitude  $\varepsilon$  at a simplified evaluation was 0.3%, as obtained from the Ramberg-Osgood equation, corresponding to the maximum elastic stress obtained by the FEM. The calculation results for the  $J$ -integral are shown in Table 1. Also, the comparison with a detailed FEM analytical result of an elbow about a short crack ( $a/c = 1/2.5$ ) is shown in Fig. 10, and about a hypothetical long crack ( $a/c = 1/55$ ) is shown in Fig. 11. The  $J$ -integral obtained by a simplified estimation method and by the FEM for the elbow agree in the case of a short crack, as seem to be shown in Fig. 10. It was confirmed from these models that the simplified estimation method that a bending takes a cracked part in the elbow, in the case of a short crack. The propagation tendency agrees with that shown in Fig. 11. In the case of a hypothetical long crack ( $a/c = 1/55$ ), the  $J$ -integral calculated by the simplified estimation method does not agree closely with that obtained by the FEM. The cause of this discrepancy lies in the use, with the simplified method of an application range outside the FEM analytic results.

### 4. Comparison with experimental results

A schematic drawing of the experimental set up of the elbow is shown in Fig. 12. The elbow specimen had a 165.2 mm outside diameter, a 152.4 mm radius of curvature, and a 4 mm wall thickness. The initial surface crack was introduced to the outer surface by electric discharge machining. The geometry of a crack created axially on the crown was rectangular, 0.7 mm in depth, and 100 mm in length. The elbow specimen was similar 1/6 scale model of the FEM model. The elbow specimen was heated in an electric furnace and was loaded with cyclic in-plane bending load by controlling the displacement of the actuator. The strain range was 0.4% as measured by means of an electric capacitance-type strain sensor with a gauge length of 2.0 mm. The test temperature was 650°C and the crack propagation length was measured by the beach mark method. Fig. 13 shows a schematic drawing of the fractured surface after testing of the elbow specimen. The crack propagated only in the direction of depth and very little in the direction of crack length. This experimental result showed good agreement with both FEM analysis and simplified estimation equation results, as shown in Figs. 14 and 15.

5. Conclusion

For the elbow with a surface crack created axially on the crown and subjected to an in-plane bending load, the  $J$ -integral and creep  $J'$ -integral were calculated by detailed 3D FEM analysis and the following conclusions were obtained, compared to a similar experiment and calculation results using a simplified estimation method.

- (1) In the case of a short crack ( $a/c = 1/2.5$ ), the  $J$ -integral of crack length direction  $J_c$  and depth direction  $J_a$  were almost the same. Therefore, good simulation crack propagation can be obtained by the simplified estimation method.
- (2) In the case of a hypothetical long crack ( $a/c \approx 1/55$ ), the  $J$ -integral of crack length direction  $J_c$  is very small compared with that of depth direction  $J_a$ . An experiment of crack propagation behavior on a 1/6 scale model agreed with the aforementioned analytic result. Crack propagation behaviors relating to this configuration could simulated by the simplified estimation method.

6. Acknowledgment

This study was performed as a part of joint research and development projects for DFBR under the sponsorship of nine Japanese electric power companies, the Electric Power Development Co., Ltd. and the Japan Atomic Power Company.

7. Reference

- (1) H. Doi et al., "Structural Analysis of Elbow with Surface Crack", Proceedings of ASME PV&P conf. (1990)
- (2) H. Wada et al., "Evaluation Method on LBB for the Piping of the DFBR", Proceedings of ASME/JSME conf. (1995)
- (3) P. Huang et al., "Simplified Estimation Equations of  $J$ -Integral for Surface Crack Under Bending Loads" (in Japanese), trans. of JSME Vol. 554 (1992)
- (4) N. Saito et al., "Development of High-Speed Analysis Program SIMUS", trans. of JSME, Vol. 53, No. 495

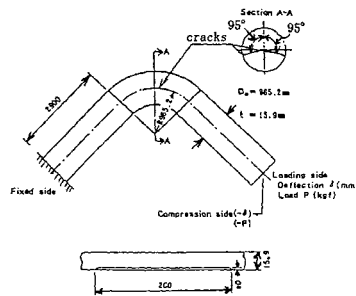


Fig. 1 Elastic-plastic and creep analyses model

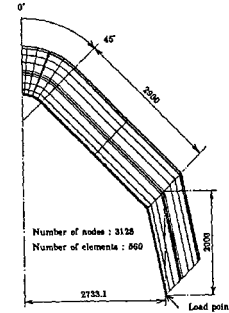


Fig. 2 Finite element mesh (Example of Case No.4)

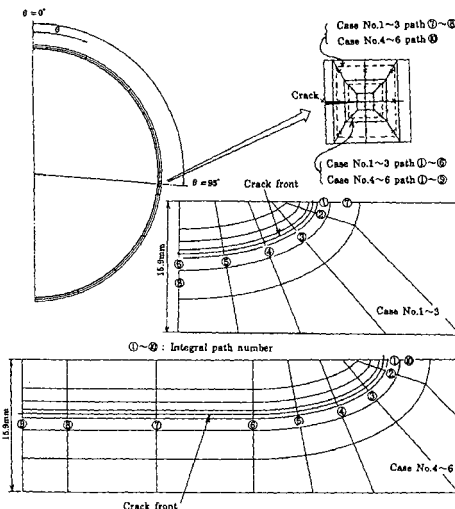


Fig. 3 Finite element mesh and integral path for  $J$  integral (VCE method)

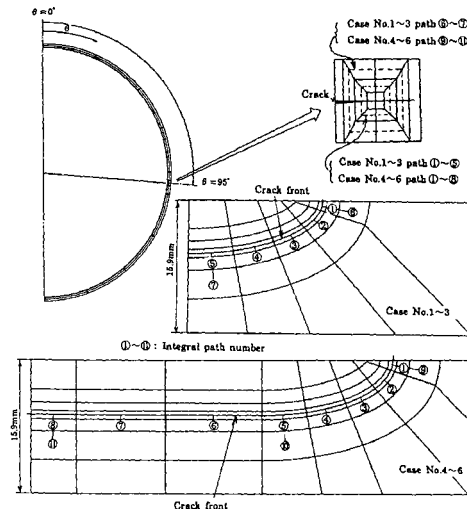


Fig. 4 Finite element mesh and integral path for  $J'$  integral

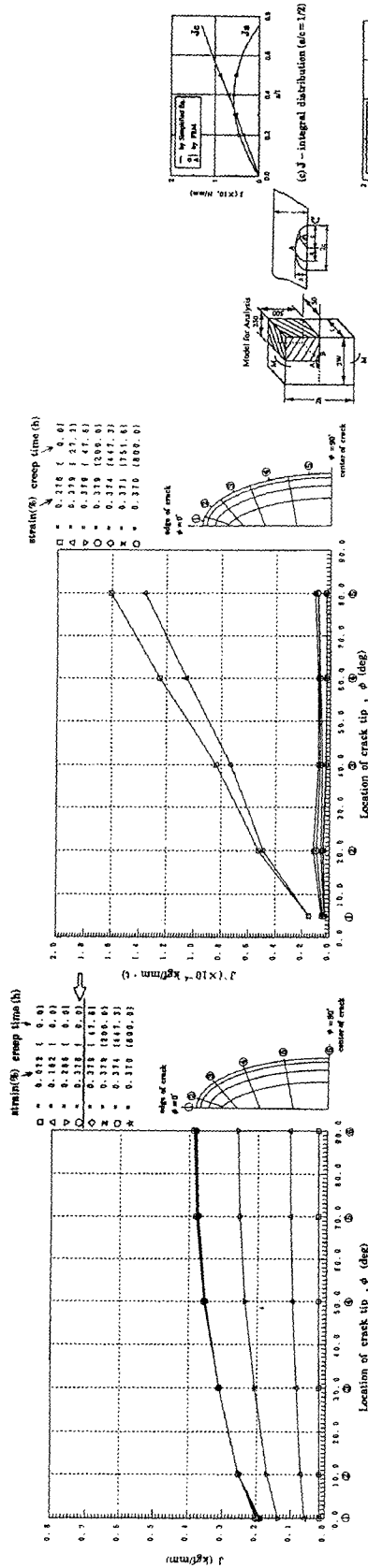


Fig. 5 J - integral distribution along crack front (Example of Case No.1)

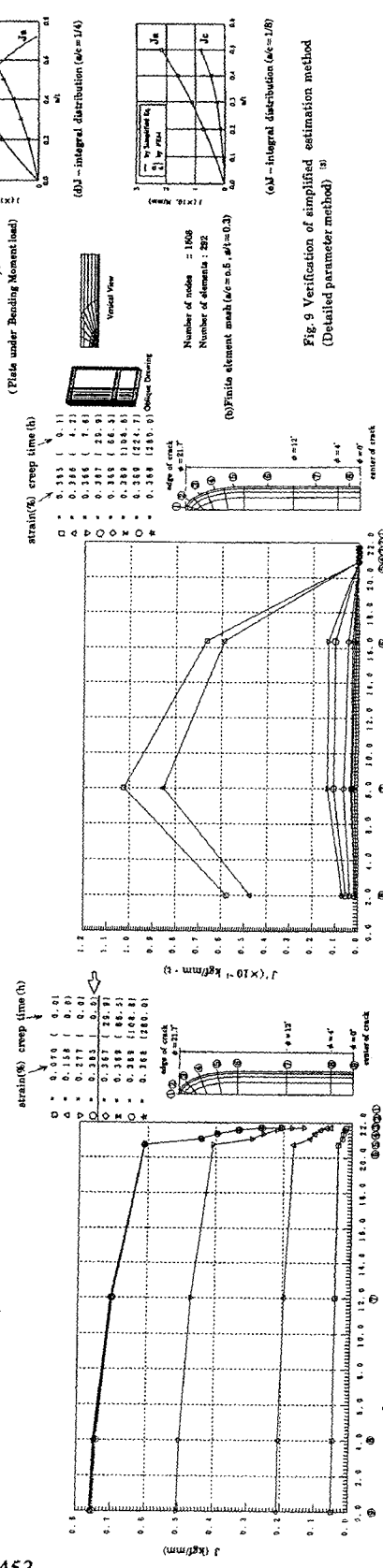


Fig. 6 J - integral distribution along crack front (Example of Case No.4)

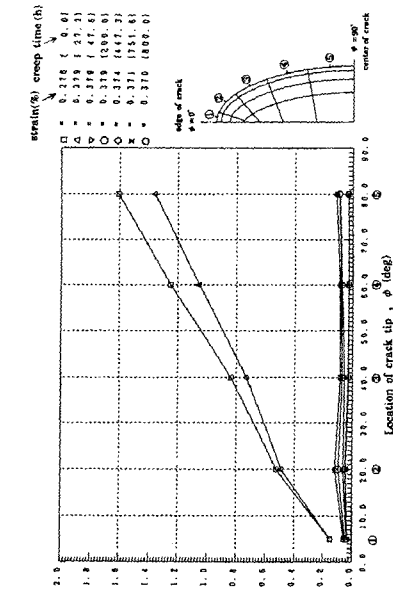


Fig. 7 Creep  $J_c$  - integral distribution along crack front (Example of Case No.1)

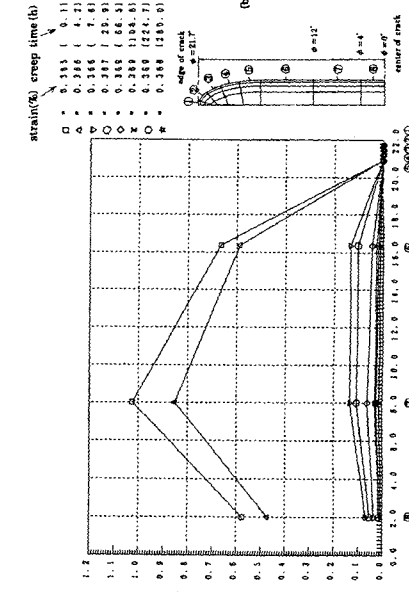


Fig. 8 Creep  $J_c$  - integral distribution along crack front (Example of Case No.4)

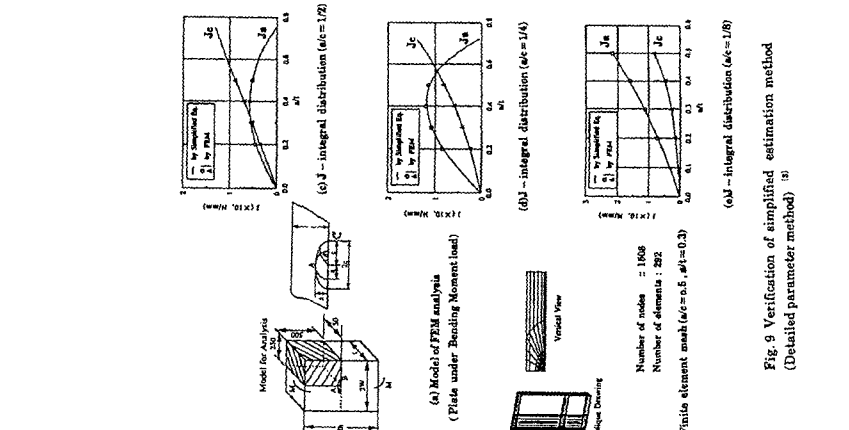


Fig. 9 Verification of simplified estimation method (Detailed parameter method)

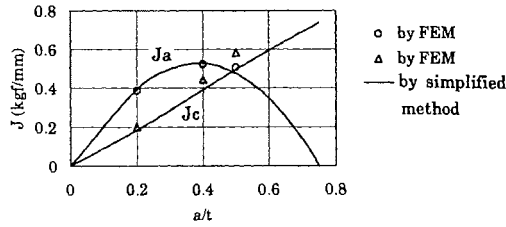


Fig. 10 Comparison of J-integral by FEM with by simplified eq. (small crack in elbow:  $a/c=1/2.5$ )

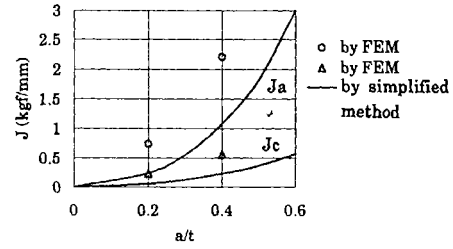


Fig. 11 Comparison of J-integral by FEM with by simplified eq. (long crack in elbow;  $a/c=1/55$ )

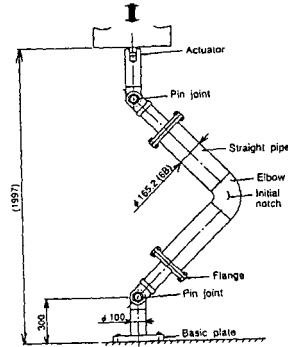


Fig. 12 Schematic drawing of experimental set up of elbow <sup>(2)</sup>

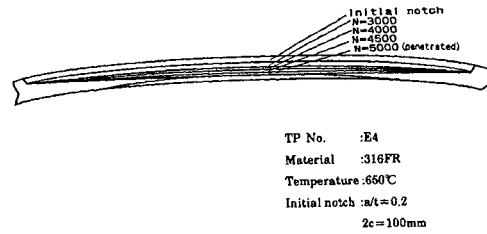


Fig. 13 Crack front propagation result in elbow under cyclic bending load ( $a_0 / c_0 = 1/70$ ) <sup>(2)</sup>

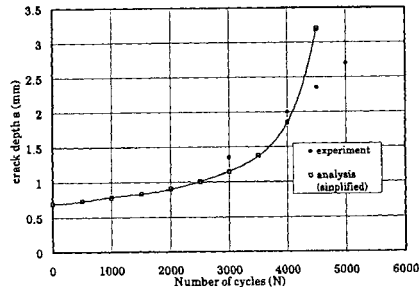


Fig. 14 Comparison of analytical and experimental crack depth ( $a_0 / c_0 = 1/70$ ) <sup>(2)</sup>

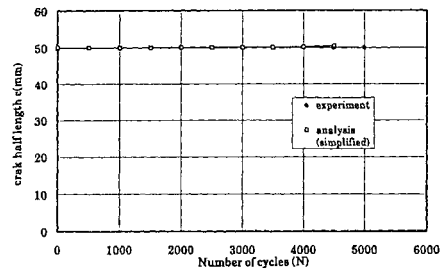


Fig. 15 Comparison of analytical and experimental crack half length ( $a_0 / c_0 = 1/70$ ) <sup>(2)</sup>

Table 1. Analytical results of J-integral values by FEM and simplified method

Case No.	Crack shape		Aspect ratio(a/c)	Method	J-integral value	
	Length(2c)	Depth(a)			Ja(kgf/mm)	Jc(kgf/mm)
1	15.9 mm	3.2mm	1/2.5	FEM	0.386	0.200
				Simplified	0.392	0.184
2	31.8 mm	6.4mm	1/2.5	FEM	0.524	0.442
				Simplified	0.527	0.391
3	39.75mm	8.0mm	1/2.5	FEM	0.508	0.581
				Simplified	0.475	0.495
4	700.0mm	3.2mm	≈ 1/109	FEM	0.752	0.208
				Simplified	0.219	0.053
5	700.0mm	6.4mm	≈ 1/55	FEM	2.206	0.560
				Simplified	1.079	0.226
6	350.0mm	3.2mm	≈ 1/55	FEM	0.738	0.227
				Simplified	0.242	0.057